The use of global navigation satellite systems for deformation analysis of the Dargovských hrdinov housing estate

Pavel Kukučka[1], ***Slavomír Labant*** *and* ***Gabriel Weiss***

In this paper, the deformation analysis of the Dargovských hrdinov housing estate using global navigation satellite systems is described. Theoretically, it deals with the reasons of formation of slope deformations, the ways of their measurement, and with the recent development and availability of GNSS. Particular attention is paid to the description of the deformation analysis technique, beginning with working out the project, locating by the GNSS, up to processing and testing of the deformation network. The practical part is based on the theoretical knowledge and describes the measurement procedure, the equipment used, working methodology and testing of the bonding network. Based on the results obtained by the deformation analysis, the paper offers information about the recent condition of the investigated area.

Key words: *deformational analysis, global navigation satellite systems, GMM*

Introduction

The global navigation satellite systems (GNSS) are increasingly used to monitor landslide areas for the needs of deformation analysis. The advantage of these measurements is mainly in their high reliability and accuracy, as well as their independence from the season and time of measurements. The main advantage is in elimination of the necessity of direct visibility between the points which is ,however, replaced by the necessity of satisfactory reception of the signal from GNSS satellites. The only condition is direct access of satellite signals at the measured points. The highest accuracy of using GNSS is achieved by relative measurements of the phase of a carrier wave. Static relative-phase measurement is a basic and most often used method in geodesy. Over the last decade, GNSS have essentially increased their accuracy that is a precondition for their use also in the field of engineering geodesy for determining shifts of building structures and slope deformations. Slope deformations are processes in which, for different reasons, the stabilty of rock slopes is affected resulting in the sliding movement of rock masses. They pose a danger to all the planned and accomplished structures whether we are talking about people‘ s dwellings or buildings which make our life on this planet easier. A slope is prone to slide due to its geological structure, properties of rocks, hydrogeological conditions, etc. The cause of slope movements is gravitation. The most important passive force is the compactness of rock.

At present 4 GNSS systems are in use or being developed (www1):

- Global Positioning System (GPS NAVSTAR),
- Global navigation Satellite System (GLONASS),
- Galileo - a system being built by the EU with global coverage by the year 2014,
- Compass - an independent system being developed by China with global coverage by the year 2017.

In Slovakia, there are 2 networks in operation which are used for spatial determining of position: SKPOS and Leica SmartNet. SKPOS is a permanent service consisting of the network of reference stations that processes and in real time provides geocentric coordinates for precise location of objects and phenomena. The reference stations receiving GNSS signals are positioned in geodetic points. The points are mainly placed on the roofs of the buildings of Land registries which are connected to the department virtual private network (VPS) to provide high quality electronic communication. In the year 2010, other 3 reference stations SKVT (Vranov nad Topľou), BREZ (Brezno), JABO (Jaslovské Bohunice) became available, thus increasing the total number of reference stations to 26. (www2, www3)

Leica SmartNet is an integrated software package that enables to centrally control and operate individual reference stations or the whole networks of reference stations. This network is a modular system with new advanced solutions for high-accuracy RTK networks with extensive coverage, centralized distribution of data and administration of data access. At present, the network includes 20 reference stations. In comparison with SKPOS that uses the technology of Virtual reference stations (VRS), the Leica SmartNet network uses MAC

[1] *Ing. Pavel Kukučka, Ing. Slavomír Labant, PhD., prof. Ing. Gabriel Weiss, PhD.*, Technical univerzity of Košice, Faculty of mining, ecology, procces control, and geotechnology, Institute of Geodesy, Cartography and Geographic Information Systems, Park Komenského 19, 040 01 Košice, Slovak Republic, pavel.kukucka@tuke.sk , slavomir.labant@tuke.sk , gabriel.weiss@tuke.sk .

(Master Auxiliary Concept) which is a newer technology. Moreover, MAC network solution provides homogenous accuracy independent from the distance from the reference station. (www4).

Location of deformation

The Dargovských hrdinov housing estate, also known as Furča is part of the town of Košice located in the district Košice III and is an independent cadastral area with acreage of 1109 hectares. The housing estate stretches in the Košice basin on the top of a major morphological elevation between the valley of the River Hornád in the west and the Torysa River in the east. The area in question (Fig. 1) is demarcated by the roads Prešovská cesta, Sečovská cesta, the streets Trieda armádneho generála L. Svobodu and Herlianska. It is situated in the Košice basin in the sub-unit of the Toryska hilly land and lies 210 – 280 m above the sea level. Located in the area there can be found the Opátsky fault (of the Zemplinsko-Berehovsky system) that runs along the foothill of the western front slopes as well as of the Hornad system, i.e. western Kosice fault and Kostoľanský fault.

The area lies in the warm climatic zone T3 with average annual temperatures varying from + 8.5 to 8.9 °C and with on average 118 frost days per year , and average depth of soil freezing 111 cm. According to SHMU measurements, the average long-term total amount of rainfall is 580 – 660 mm.

Fig. 1. Area map.

Measurement of the network and evaluation of signals

Measurements were performed using two types of double-frequency receivers Leica GPS900CS, Leica GPS1200 and a digital levelling device Topcon DL-101C. Leica GPS1200 (Fig. 2) and Leica GPS900CS (Fig. 3) are double-frequency geodetic RTK receivers that allow to use static, fast static, kinematic and On the fly methods for measurements. Topcon DL-101C allows to perform the levelling measurement using the method of technical, precise and very accurate levelling as well as laying-out.

Fig. 2. Measuring at the point Haringeš.

Prior to the measurement itself, thorough reconnaissance of the terrain was carried out in order to investigate the condition of the point field and select suitable observed points (hereinafter OP) in the risky areas. After the reconnaissance, it was found out that in the area there were a lot of points serving for assessment of slope movements, however, some of these points were reconstructed and some of them were destroyed. All the points were stabilized as interconnected geodetic points (lined drilled wells fitted with a metal pipe and filled with concrete). On the surface of each pillar there was cemented a metal plate with a drilled hole 16 mm in diameter which provided dependent centring and the benchmark was fitted at the lower part of the pillars (Fig. 3).

The choice of suitable OP in the risky areas was dependent on the density of the built-up area and vegetation cover. 5 OP marked B -6, B-10, C-20, P-III-1, P-IV-1 (Fig. 4) were selected for monitoring slope deformations stabilized with the lined drilled wells where there was an increased anticipation of movement. Selection of these points was performed taking into consideration the option of the best possible reception of signals from the satellites. Haringeš,

Fig. 3. Measuring at the point P-IV-1.

Varkapa and Široká points were used for processing as reference points (hereinafter marked as H, V, S) stabilized by nailed signs with holes in stone prisms of the size 20 x 20 x 70 cm protected by concrete rings and protective rods (Fig. 2). (Sabova, 2007, AMS)

Before the experimental measurement, which was performed on 13 June 2009, a suitable method of measurement was selected to ensure the highest accuracy of observation. The selected method appropriate for the intended measurement was a static method with 3 pieces of Leica GPS1200 equipment and 5 pieces of Leica GPS900CS equipment (+1 back-up) available to carry out the measurement. The difference between these types of equipment, apart from their technical parameters, lies mainly in the fact that Leica GPS1200 receives only GPS signals and Leica GPS900CS allows to receive signals from the GPS satellite system as well as from GLONASS (GNSS receiver). That's because of this very difference that the positioning of the equipment was reassessed with the conclusion that GPS (Leica GPS1200) receivers should be installed on the reference points (hereinafter RP) H, V, S, where the sky was not blocked and a smaller number of observation satellites would be required. GNSS (Leica GPS900CS) receivers were positioned on the OP where a clear view of the sky is sometimes limited and it was necessary to increase the number of observation satellites. In this case these were GLONASS satellites that were used.

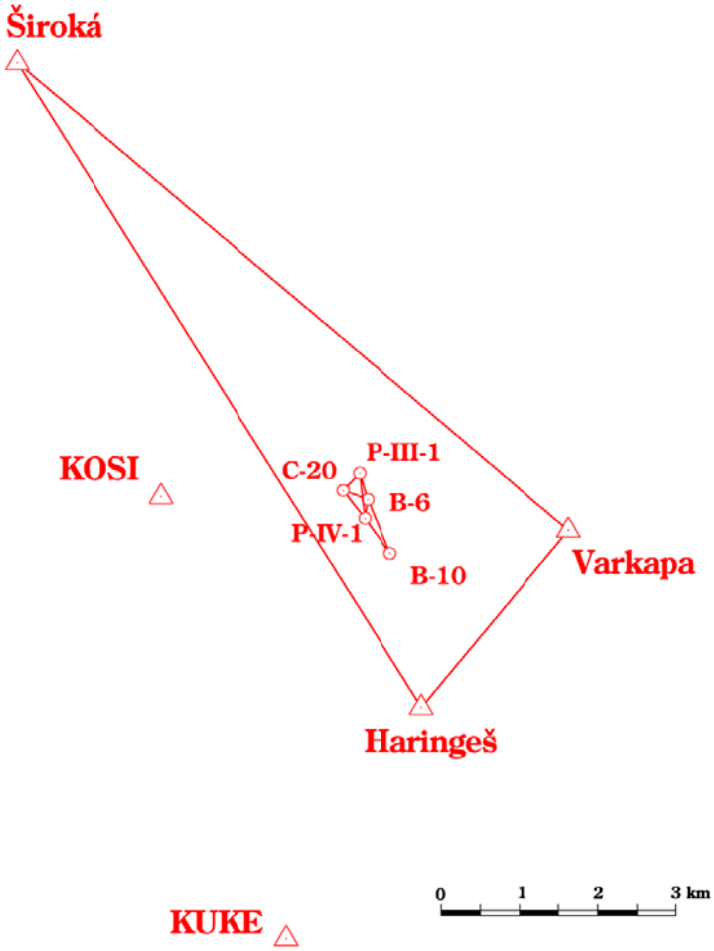

Fig. 4. Situation of the deformation networks.

Before the measurement it was necessary to set the same mode of measurement for every piece of equipment to avoid distortion of the results of the measurements due to the wrong setting. Leica GPS900CS equipment was positioned on all of the OP using a Zeiss pad and two types of fixing bolts. A clamp bolt was used for gripping of the Zeiss pad to the pillar thus providing vertical centring; the second one was used for gripping of the antenna in the Zeiss pad. Levelling was performed using pre-rectified optical centring device imbedded into the Zeiss pad. Receivers Leica GPS1200 were positioned on the RP on tripods with three telescopic legs using the Zeiss pad and a special bolt. A rectified optical centring device was used for levelling the devices.

During the observation, the height difference of the receivers' antennas and benchmarks of the points was determined by the levelling method using a digital levelling device Topcon DL–101C. For each measurement the horizontal position was adjusted so that the horizontal adjustment line in the telescope of the levelling device was the same as the height determined on the antenna (Fig.5) and consequently the height was electronically read off several times for more precise adjustment on the code levelling lath placed on the benchmark of the point. The resulting height was calculated on the basis of the arithmetical average. The control measurement of the slant distance was performed by applying an additional measuring tape to compare or eventually detect gross errors. 4-hour observations were recorded at all points with the time of measurement from 11:00 - 15:00.

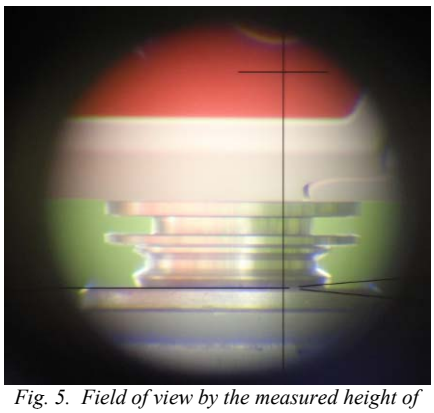

Fig. 5. Field of view by the measured height of antenna.

Processing of the measured data was carried out using the company software Leica Geo Office 5.0 (LGO) where the fact was taken into account that in the area of the town of Košice there were RP of two independent from each other permanent GNSS services, namely KUKE reference station of SKPOS servive placed on the building of the Land registry in Košice and KOSI reference station of Leica SmartNet network placed on Delliuss pavilion on the campus of the Technical University. The data from the reference stations for the given time of measurement were received from Ms Šalátová (data from KUKE) and from Mr E. Frohmanna, PhD (data from KOSI) upon written requests in the exchange format RINEX.

In order to compare the point position determined by SKPOS and Leica SmartNet service, in the software processing it was always only one point was chosen as a RP from the pair of KUKE and KOSI points and the other was not used so that two independent sets of the coordinates of the OP in the coordinate system Unified Trigonometric Cadastral Network 03 (UTCN 03) were obtained. By comparison of the individual sets of coordinates it was proved that the data provided by the state permanent service of SKPOS observation stations and the private Leica SmartNet network were at the same accuracy level (Tab. 1).

Tab. 1. Differences of coordinates of points.

number of points		KUKE SKPOS [m]	KOSI SmartNet [m]	coordinate differences [mm]
B-6	X	1238170.736	1238170.736	-0.01
	Y	261135.932	261135.932	0.04
	Z	245.954	245.954	0.00
B-10	X	1238862.019	1238862.019	0.05
	Y	260850.333	260850.333	-0.02
	Z	280.352	280.352	0.00
C-20	X	1238054.799	1238054.799	-0.01
	Y	261450.470	261450.470	0.04
	Z	218.245	218.245	0.00
P-III-1	X	1237837.328	1237837.328	-0.03
	Y	261238.307	261238.307	-0.03
	Z	260.160	260.160	0.00
P-IV-1	X	1238412.352	1238412.352	0.01
	Y	261173.400	261173.400	-0.02
	Z	265.198	265.198	0.00

For the purposes of the deformation analysis performed independent processing of the bonding network was performed which corresponded to processing in the year 2003 when the position of the points was carried out using the GNSS method and the height was determined using the hight precision levelling (HPL) method. In the year 2003 the points H, V, S were used as RP and because of that for the year 2009 the KOSi and KUKE points were excluded from processing. In the year 2003, the HPL method was used to determine the heights of the points using the levelling device Zeiss Ni 007 with an average kilometer error 0,5 mm/km and in the year 2009 determination of the heights was carried out using the GNSS static method with the vertical position determination 10 mm + 0.5 D ppm.

As the yearly measurements did not have the same precision level, and the initial comparison of heights by the GNSS method with the year 2003 showed considerable differences, processing of the 3D network was cancelled, in which significant height differences negatively affected the overall results, and only positioning processing of the bonding network was carried out. Initial pre-processing of the observation data was performed in LGO 5.0 software environment where, for the sake of updating, transformation of the coordinates of the OP and RP from the coordinate system ETRS 89 into the local coordinate system UTCN 03 (Unified Trigonometric Cadastral Network 03) was carried out using the transformation parameters UTCN 03. Transformation of the year 2003 used for the deformation analysis was performed using similar transformation (Šütti, 1997), where on the basis on the respective formulas the accuracy of the transformation of individual coordinates of the OP was determined with an average value of the mean error of the transformation 17.68 mm.

Gauss-Markov model with full rank

Positioning coordinates of 5 OP and 3 RP as well coordinate differences between them (Fig. 5) were used for 2D bonding processing of the estimates of unknown parameters using Gauss-Markov model (GMM) given by:

$$\begin{aligned} v &= Ad\hat{C} - dL = A(\hat{C} - C^{\circ}) - (L - L^{\circ}), && \text{- functional part,} \\ \Sigma_L &= s_0^2 Q_L, && \text{- stochastic part,} \end{aligned} \qquad (1)$$

The structure of individual values in this network is defined by $m = 25$ GNSS vectors obtained through observations, $n = 2m = 50$ observation components, $b = 8$ OP and $k = 2b = 16$ determined by parameters, with $k = 10$ being only for the OP. (Gašinec et al., 2000; Pukanská et al., 2007, Sabová et al., 2007; Weiss et al., 2008):

Vector of observations $L_{(50,1)}$ is created by position coordinate differences between individual network points which are taken from the processing of vector in LGO 5.0 software. The sequence of coordinate differences is given in alphabetical order of vector starting points based firstly on observed points and then on RP with coordinate differences ΔX , ΔY . This order is maintained for the entire adjustment.

A vector of approximate coordinates of OP $C^{\circ}_{(10,1)}$ is created by position coordinates of OP, which were taken from initial processing in LGO 5.0 software.

A vector of approximate observations $L^{\circ}_{(50,1)}$ is given by relative coordinate differences of approximate coordinates of given points $L^{\circ} = f(C^{\circ})$. The order of individual differences is the same as in vector of observations L.

The vector of observation additives $dL_{(50,1)}$ is given by the difference of the elements of the observation vector and the vector of approximate observations : $dL = L - L^{\circ}$ and is determined in milimetres.

Cofactor matrix $Q_{L\,(50,50)}$ is a diagonal matrix with cofactors on the main diagonal. Individual cofactors were calculated from the relationship $q_i = \frac{\sigma_i^2}{\sigma_0^2}$, where $\sigma_0^2 = \frac{\Sigma \sigma_{\Delta X, \Delta Y}{}^2}{n}$, $\sigma_i^2 = (5mm + 0.5ppm)^2$ and the accuracy of the determination of the length of individual vectors using the static method quoted by the manufacturer is 5 mm + 0,5 mm/km of the length.

Configuration matrix A (partial derivations, design) characterises network geometry (configuration) of the network. As there were 3 RP in the given network, the matrix $A_{(50,16)}$ was divided into active part $A_{(50,10)}$, which was further processed and passive part $A_{(50,6)}$, which belonged to 3 RP and was defined as: $A = \left(\frac{\partial f(C^{\circ})}{\partial C^{\circ}} \right)_{C^{\circ}=\hat{C}}$. If vectors L° and C° are related to each other, the coefficients will have values $\{-1,1\}$ and if not, they will have value $\{0\}$.

Vector of estimates of auxiliaries of determined coordinates $d\hat{C}_{(10,1}$ in mm was determined using a matrix multiplication:

$$d\hat{C} = (A^T Q_L^{-1} A)^{-1} A^T Q_L^{-1} (L - L^{\circ}) = N^{-1} A^T Q_L^{-1} dL . \qquad (2)$$

The vector of adjusted coordinates of the OP $\hat{C}_{(10,1)}$ is determined by addition of the vector of approximate coordinates C^{o} and the vector of estimates of coordinate additives for the calculated points $d\hat{C}$:

$$\hat{C} = C^{\circ} + d\hat{C} . \qquad (3)$$

Vector of corrections $v_{(50,1)}$ of observed values: $v = Ad\hat{C} - dL$. (4)

Vector of adjusted measured values $\hat{L}_{(50,1)}$: $\hat{L} = L + v$. (5)

Estimated variance faktor $s_{0\,(1,1)}^2$: $s_0^2 = \frac{v^T Q_L^{-1} v}{(n-k)}$. (6)

The covariance matrix $\Sigma_{\hat{C}\,(10,10)}$ of adjusted coordinates $\hat{X}_i, \hat{Y}_i$ observed points is: $\Sigma_{\hat{C}} = s_0^2 Q_{\hat{C}}$ (7)

where on the main diagonal there are variances showing the accuracy of the estimates of the calculated coordinates.

Covariance matrix of the adjusted values of the observed quantities is $\Sigma_{\hat{L}\,(50,50)}$: $\Sigma_{\hat{L}} = s_0^2 Q_{\hat{L}}$ (8)

Redundancy matrix $R_{(50,50)}$ is the product of cofactor matrix Q_L and cofactor matrix of corrections Q_V :

$$R = Q_V Q_L^{-1} = (Q_L - AN^{-1}A^T) Q_L^{-1} . \qquad (9)$$

Table 2 shows measured, approximate and adjusted numerical data that relate to the measured values having vector size (50,1) giving units of quantities. The total of the elements on the main diagonal of the redundancy matrix fulfills the equation given by the relationship to the redundancies of the network:

$$tr(R) = r_1 + r_2 + ... + r_n = \sum_{i=1}^{n} r_1 = r = n - k = 50 - 10 = 40.$$

Table 3 contains approximate and adjusted numerical data that relate to the determined coordinates of the size of vectors (10,1) given with the units of individual quantities.

Tab. 3. Coordinates of OP and their accuracy.

Points coordinates	$C^{\circ}_{(10,1)}$	$d\hat{C}_{(10,1)}$	$\hat{C}_{(10,1)}$	$\sigma_{\hat{C}\,(10,1)}$
	[m]	[mm]	[m]	[mm]
X_{B-6}	1238170.732	-0.39	1238170.732	0.37
Y_{B-6}	261135.927	0.38	261135.927	0.38
X_{B-10}	1238862.015	0.12	1238862.015	0.40
Y_{B-10}	260850.322	0.66	260850.323	0.42
X_{C-20}	1238054.795	-0.14	1238054.795	0.38
Y_{C-20}	261450.467	-0.39	261450.467	0.38
$X_{P-III-1}$	1237837.321	-0.61	1237837.320	0.38
$Y_{P-III-1}$	261238.302	0.11	261238.302	0.38
X_{P-IV-1}	1238412.354	-1.44	1238412.353	0.38
Y_{P-IV-1}	261173.393	-0.02	261173.393	0.39

After processing the measured quantities it was necessary to verify by statistical testing if in the vector of the measured values there were any measurements containing gross errors.

Tab. 2. Measured data and their accuracy.

GNSS vector			$L_{(50,1)}$	$L^{\circ}_{(50,1)}$	$dL_{(50,1)}$	main diag. $Q_{L\ (50,1)}$	$v_{(50,1)}$	$\hat{L}_{(50,1)}$	$\sigma_{\hat{L}\ (50,1)}$	main diag. $R_{(50,1)}$
from point	to point	ΔX/ΔY	[m]	[m]	[mm]		[mm]	[m]	[mm]	
B-6	B-10	Δ X	691.283	691.283	0.00	0.632	0.51	691.284	0.44	0.71
		Δ Y	-285.605	-285.605	0.50	0.546	-0.22	-285.605	0.43	0.67
B-6	C-20	Δ X	-115.936	-115.937	1.00	0.511	-0.75	-115.937	0.41	0.68
		Δ Y	314.539	314.540	-0.50	0.552	-0.27	314.539	0.41	0.70
B-6	P-III-1	Δ X	-333.412	-333.411	-0.50	0.555	0.27	-333.411	0.42	0.69
		Δ Y	102.375	102.375	0.00	0.508	-0.26	102.375	0.40	0.69
B-6	P-IV-1	Δ X	241.622	241.622	-0.50	0.536	-0.55	241.621	0.42	0.69
		Δ Y	37.465	37.466	-1.00	0.496	0.61	37.466	0.41	0.67
B-6	H	Δ X	2655.899	2655.899	0.00	1.145	0.39	2655.899	0.37	0.72
		Δ Y	-687.223	-687.222	-1.00	0.632	0.62	-687.222	0.38	0.70
B-6	S	Δ X	-5566.742	-5566.742	0.00	2.180	0.39	-5566.742	0.37	0.73
		Δ Y	4468.873	4468.871	2.00	1.751	-2.38	4468.871	0.38	0.68
B-6	V	Δ X	395.189	395.189	0.00	0.568	0.39	395.189	0.37	0.68
		Δ Y	-2568.787	-2568.786	-1.00	1.119	0.62	-2568.786	0.38	0.67
B-10	C-20	Δ X	-807.221	-807.220	-1.00	0.659	0.74	-807.220	0.44	0.68
		Δ Y	600.144	600.145	-1.00	0.612	-0.05	600.144	0.44	0.69
B-10	P-III-1	Δ X	-1024.694	-1024.694	0.00	0.709	-0.73	-1024.695	0.45	0.70
		Δ Y	387.981	387.980	0.50	0.567	-1.04	387.979	0.43	0.69
B-10	P-IV-1	Δ X	-449.663	-449.661	-2.00	0.580	0.44	-449.663	0.44	0.71
		Δ Y	323.069	323.071	-2.00	0.553	1.33	323.070	0.43	0.68
B-10	S	Δ X	-6258.025	-6258.025	-0.50	2.475	0.38	-6258.025	0.40	0.88
		Δ Y	4754.479	4754.476	2.50	1.858	-3.16	4754.475	0.42	0.78
B-10	V	Δ X	-296.094	-296.094	0.00	0.548	-0.12	-296.094	0.40	0.94
		Δ Y	-2283.183	-2283.181	-1.50	1.036	0.84	-2283.182	0.42	0.92
C-20	P-III-1	Δ X	-217.474	-217.474	0.00	0.532	-0.47	-217.474	0.42	0.76
		Δ Y	-212.164	-212.165	1.00	0.530	-0.50	-212.164	0.41	0.88
C-20	P-IV-1	Δ X	357.557	357.559	-1.50	0.560	0.20	357.558	0.42	0.94
		Δ Y	-277.073	-277.074	0.50	0.544	-0.13	-277.074	0.42	0.91
C-20	H	Δ X	2771.836	2771.836	0.00	1.179	0.14	2771.836	0.38	0.71
		Δ Y	-1001.762	-1001.762	0.00	0.703	0.39	-1001.762	0.38	0.83
C-20	S	Δ X	-5450.804	-5450.805	0.50	2.133	-0.36	-5450.805	0.38	0.88
		Δ Y	4154.333	4154.331	1.50	1.636	-1.11	4154.331	0.38	0.80
C-20	V	Δ X	511.126	511.126	0.00	0.593	0.14	511.126	0.38	0.94
		Δ Y	-2883.327	-2883.326	-0.50	1.214	0.89	-2883.326	0.38	0.91
P-III-1	P-IV-1	Δ X	-575.033	-575.033	0.50	0.607	-1.32	-575.034	0.43	0.77
		Δ Y	64.910	64.909	1.50	0.501	-1.63	64.909	0.41	0.88
P-III-1	H	Δ X	2989.309	2989.310	-1.00	1.246	1.61	2989.311	0.38	0.89
		Δ Y	-789.597	-789.597	0.00	0.655	-0.11	-789.597	0.38	0.79
P-III-1	S	Δ X	-5233.331	-5233.331	0.50	2.045	0.11	-5233.330	0.38	0.93
		Δ Y	4366.497	4366.496	1.00	1.713	-1.11	4366.496	0.38	0.92
P-III-1	V	Δ X	728.601	728.600	1.00	0.641	-0.39	728.601	0.38	0.78
		Δ Y	-2671.162	-2671.161	-1.00	1.149	0.89	-2671.161	0.38	0.88
P-IV-1	H	Δ X	2414.279	2414.277	2.50	1.073	-1.06	2414.278	0.38	0.87
		Δ Y	-724.688	-724.688	0.50	0.640	-0.48	-724.688	0.39	0.77
P-IV-1	S	Δ X	153.569	153.567	2.00	0.519	-0.56	153.568	0.38	0.73
		Δ Y	-2606.253	-2606.252	-1.00	1.130	1.02	-2606.252	0.39	0.87
H	V	Δ X	-2260.709	-2260.710	0.50	1.029	-0.50	-2260.710	0.00	1.00
		Δ Y	-1881.564	-1881.564	0.00	0.925	0.00	-1881.564	0.00	1.00
S	V	Δ X	5961.931	5961.931	-0.50	2.346	0.50	5961.931	0.00	1.00
		Δ Y	-7037.659	-7037.657	-2.50	2.830	2.50	-7037.657	0.00	1.00

Testing of the network

The adjusted network structure was tested using various methods. Suitability of selection of GMM used for adjustment was verified by a global test of an estimating model and the presence of remote measurements was tested by a Pope Tau method, Krűger's test and testing of diverged values.

In the global test, test statistics T given by the calculation $T = \frac{s_0^2}{\sigma_0^2}(n-k) = 0{,}806$ was compared with the critical value with division χ^2 (chi-Square) at the level of significance $\alpha = 0{,}05$ and grades of freedom $f = (n-k)$: $\chi_\alpha^2(n-k) = 1{,}484$ where $n = 2m = 50$ represents the number of observation components and $k = 2b = 10$ represents the number of determined parameters.

As the critical value was higher than the testing criterion $\chi_\alpha^2 > T$, the test did not confirm any differences between the mathematical model of processing and the observations used, therefore it can be considered as not distorted and observations as not containing gross errors. (Caspary, 1987)

Deformation analysis

Assessment of changes in the area in question in the mid period t_i and t_{i+1} was carried out based on changes in the coordinates of the points in the given area. Since, as the result of carrying out bonding processing of the network the coordinates of the OP - B-6, B-10, C-20, P-III-1 and P-IV-1 in the UTCN system for the year 2009 were adjusted, the deformation analysis was performed. The stability of the given points in the period between the years 2003 and 2009 was investi-gated. Through compa-rison of the adjusted coordinates of the OP in the years 2003 and 2009 the deformation vector was determined given by:

Tab. 4. Testing of the networks with local tests.

from point	to point	Pope Tau method			Krűger's test			testing of diverged values		
		TKRIT	TXi	TYi	TKRIT	TXi	TYi	TKRIT	TXi	TYi
B-6	B-10		0.744	0.358		0.740	0.354		0.127	0.064
B-6	C-20		1.256	0.423		1.266	0.418		0.236	0.077
B-6	P-III-1		0.435	0.440		0.430	0.436		0.078	0.083
B-6	P-IV-1		0.889	1.033		0.887	1.034		0.163	0.196
B-6	H		0.380	0.871		0.376	0.868		0.054	0.157
B-6	S		0.267	1.842		0.264	1.901		0.028	0.224
B-6	V		0.580	0.618		0.575	0.613		0.108	0.088
B-10	C-20		1.063	0.070		1.065	0.069		0.180	0.012
B-10	P-III-1		1.003	1.650		1.003	1.688		0.165	0.299
B-10	P-IV-1		0.696	2.142		0.692	2.247		0.122	0.395
B-10	S		0.247	2.392		0.244	2.552		0.024	0.288
B-10	V		0.186	0.892		0.184	0.890		0.034	0.130
C-20	P-III-1	3.280	0.776	0.809	4.091	0.772	0.805	2.010	0.142	0.149
C-20	P-IV-1		0.319	0.202		0.316	0.200		0.057	0.037
C-20	H		0.135	0.512		0.133	0.507		0.019	0.088
C-20	S		0.251	0.894		0.248	0.892		0.027	0.108
C-20	V		0.204	0.846		0.202	0.843		0.037	0.117
P-III-1	P-IV-1		1.983	2.753		2.062	3.020		0.358	0.551
P-III-1	H		1.511	0.154		1.537	0.152		0.210	0.027
P-III-1	S		0.081	0.873		0.080	0.870		0.009	0.104
P-III-1	V		0.537	0.868		0.533	0.866		0.096	0.123
P-IV-1	H		1.082	0.679		1.085	0.674		0.159	0.120
P-IV-1	S		0.899	1.008		0.897	1.008		0.173	0.144
H	V		0.485	0.000		0.480	0.000		0.077	0.000
S	V		0.321	1.463		0.318	1.484		0.034	0.144

$$ {}^{t2009-2003}d\hat{C}_i = \begin{pmatrix} {}^{t2009-2003}d\hat{X} \\ {}^{t2009-2003}d\hat{Y} \\ {}^{t2009-2003}d\hat{Z} \end{pmatrix}_i = \begin{pmatrix} {}^{t2003}\hat{X} - {}^{t2009}\hat{X} \\ {}^{t2003}\hat{Y} - {}^{t2009}\hat{Y} \\ {}^{t2003}\hat{Z} - {}^{t2009}\hat{Z} \end{pmatrix}_{i,\ i=1,2,..,5} . \quad (10) $$

Table 5 gives the differences of the coordinates for all the OP. The values of these differences were up to 6 mm only for the point B-6 and P-VI-1 where the difference of coordinates in the direction of the y-axis was 16.84 mm and in the direction of the x-axis 12.92 mm. Positional shift (Fig. 6) of these points was the biggest for the points B-6 and P-VI-1 which was 17.37 mm and 14.30 mm whereas for other points it was up to 4.74 mm.

Through subsequent testing by a global test and a local test it was investigated whether coordinate differences occured through movememts of points or arose based on the errors in the measu-rements and processing.

Tab. 5. Coordinates of OP in the period of 2003 and 2009.

Bod		Epoch 2009 [m]	Epoch 2003 [m]	coordinate differences [mm]	Positional shift [mm]
B-6	X	1238170.732	1238170.736	-4.25	17.37
	Y	261135.927	261135.911	16.84	
B-10	X	1238862.015	1238862.019	-4.10	4.19
	Y	260850.323	260850.322	0.82	
C-20	X	1238054.795	1238054.798	-2.75	4.74
	Y	261450.467	261450.463	3.86	
P-III-1	X	1237837.320	1237837.317	3.43	3.45
	Y	261238.302	261238.302	0.36	
P-IV-1	X	1238412.353	1238412.365	-12.92	14.30
		26117	26117	-6.13	

The stability or instability of all the points was tested by the global test with o hypothesis $H_0 : {}^{t_{2003}}\hat{C} - {}^{t_{2009}}\hat{C} = 0$. The testing statictics $T = 0{,}419$ was compared with the critical value F - random variable T at the significance level $\alpha = 0{,}05$ and degrees of freedom $f_1 = k = 10$, $f_2 = n - k = 50 - 10$: $F_\alpha(1-\alpha, f_1, f_2) = 2{,}065$.

It is given that $T < F_\alpha$, therefore the differences of coordinates can be considered as a statistically insignificant stochastic change of the position of a point, and because of that all the OP can be considered as stable.

Though the global test did not prove the self-movement of the points, localization testing was conducted to examine the stability of individual points. For each point of the deformation network the localization testing statistics T_i was used given by the relationship:

Tab. 6 Local testing of points

points		T_i	T_{KRIT}
B-6	X	1.094	8.112
	Y	0.634	8.081
B-10	X	0.142	8.052
	Y	0.070	8.023
C-20	X	0.057	7.997
	Y	0.061	7.971
P-III-1	X	0.045	7.947
	Y	0.029	7.923
P-IV-1	X	0.002	7.901
	Y	0.001	7.880

$$T_i = \frac{d\hat{C}_i^{\,T}\; Q_{d\hat{C}_i}^{\;-1}\; d\hat{C}}{\bar{s}_0^2 k_1} \approx F_\alpha(f = k_1, f' = n - k), \quad i = (1,2,...,5) \tag{11}$$

where $k_1 = 2$ is the number of the tested parameters of the particular point which was compared with the critical value $T_{KRIT}(F_\alpha)$ (Tab. 6) at the significance level $\alpha = 0{,}05$ and degrees of freedom $f = k_1 = 2$, $f' = n - k = 50 - 10$. (Weiss et al., 2007).

From Table 6 it is obvious that in the local testing of points in all the cases the critical value was bigger than the testing criterion, hence the OP - B-6, B-10, C-20, P-III-1 a P-IV-1 as well the area defined by these points could be considered as stabile.

Graphic testing using confidence ellipses (Sabová et al., 2002) confirmed the conclu-sions drawn from global and local testing of the stability of the OP located in the Dargovských hrdinov housing estate (Fig. 6). As the positio-nal vector of the point shift in the period of the years 2003 and 2009 was located inside the confidence ellipse (Tab. 7), there was no shift and therefore it was about the accumulation of the survey errors.

Tab.7. Parameters of the relative confidence ellipses

	a [mm]	b [mm]	σ_{ui} [g]
B-6	20.49	20.45	0.00
B-10	21.36	21.09	0.00
C-20	20.6	20.46	0.00
P-III-1	20.57	20.48	0.00
P-IV-1	20.73	20.58	0.00

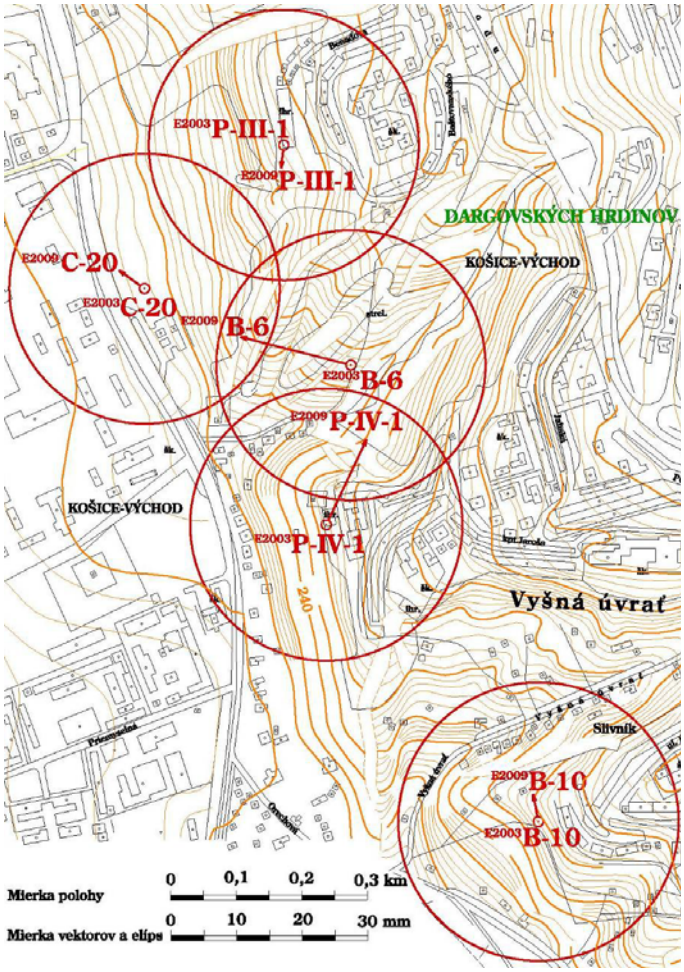

Fig. 6 Graphic testing with confidence ellipses in the period between 2003 and 2009.

If a point in the year 2009 was outside the ellipse, then we could state that there was a shift which would be supported by the statistical testing. From the conclusions of the deformation analysis it appears that in the period between the years 2002 and 2009 there occurred no shifts of points whatsoever and that coordinate differences that arose were only due to survey errors which was proven by the identification test.

Based on these conclusions, we can consider the area represented by the OP - B-6, B-10, C-20, P-III-1 and P-IV-1 as stabile, however it is necessary to further monitor this area.

Conclusion

Monitoring of landslide areas is necessary to ensure safety and identify risk factors. When monitoring it is crucial to pay particular attention to developing the project and the choice of the method of work. It is always essential to consider economic, time and accuracy criteria. The use of GNSS for the needs of deformation investigation appeared to be most useful both in terms of time, reliability and precision. The advantage of this choice was that determination of the vertical position of the points was less accurate what in case of processing the 3D deformation network would affect the overall results. For that reason it is more advisable to determine the position of the surveyed points using the method of very precise levelling. As follows from the results of the deformation analysis, coordinate differences of the surveyed points are statistically significant which is proved by the stability of the area.

References

Caspary, W. F.: Concepts of network and deformation analysis. *1st edition. Kensingthon: School of surveying The University of New South Wales, 1987. 187 p., ISBN 0-85839-044-2*.

Gašinec, J., Gašincová, S., Rajniak, M.: To the problem of the adjustment of 2D geodetic networks. In: Current issues of land surveying and engineering geodesy : proceedings from the interenational scientific seminar : Herľany, *9 – 10 October 2000, FBERG, TU Košice, pp. 38-42, 2000, ISBN 80-7099-595-5*.

Pukanská, K. and Weiss, G.: The accuracy of location points using GPS technology. Coal - Ores - Geological Survey, *14, 9, pp. 30-35, 2007, ISSN 1210-7697*.

Sabová, J., Gašincová, S.: Graphic testing in deformation monitoring. *Acta Montanistica Slovaca. Vol. 7, 2002, no. 2, pp. 127-130, ISBN 1335-1788*.

Sabová, J., Jakub, V.: Geodetic deformation monitoring. *1st edition. Košice: Editor centre and editorial office AMS, F BERG, Technical University of Košice, 2007. 128p., ISBN 978-80-8073-788-7*.

Sabová, J., Pukanská, K.: Projekt der Deformationsuntersuchungen. *Acta Montanistica Slovaca. Vol. 12, 2007, Special Issue no. 3, pp 516-519, ISBN 1335-1788*.

Šütti, J.: Deviationless geodetic transformations. *Acta Montanistica Slovaca, Vol. 2, 1997, no. 1, pp. 1-10, ISBN 1335-1788*.

Tometz, L.: Košice - Dargovských hrdinov housing estate, horizontal wells. Registered in the Archieve of the geological survey, *TUKE, 2004*.

Weiss, G., Gašinec, J., Engel, J., Labant, S., Rákay, ml., Š.: Effect incorrect points of the Local Geodetic Network at results of the adjustment. *Acta Montanistica Slovaca, Vol. 13, 2008, 4, pp. 485-490, ISBN 1335-1788.*

Weiss, G., Jakub, V.: The test verification of 3D geodetic points and their changes. *Acta Montanistica Slovaca. 12, Special Issue 3, 2007, pp. 612-616. ISSN 1335-1788*.

www1: Global navigation satelite system [online]. [cit. 2010.3.25]. Available at: http://en.wikipedia.org/wiki/Global_navigation_satellite_system

www2: Geodetic and Cartographic Institute Bratislava [online]. [cit. 2010.3.23]. Available at: http://www.gku.sk/predmet-cinnosti/geodeticke-zaklady

www3: Web server SKPOS [online]. [cit. 2010.7.15]. Available at: http://www.skpos.gku.sk/

www4: SmartNet Slovakia [online]. [cit. 2010.3.20]. Available at: http://www.geotech.sk/srv_gtch.htm